Han's model parameters for microalgae grown under intermittent illumination: Determined using particle swarm optimization

Victor Pozzobon, Patrick Perre

Journal of Theoretical Biology, DOI: 10.1016/j.jtbi.2017.10.010

Han's model parameters for microalgae grown under intermittent illumination - determined using particle swarm optimization

Victor Pozzobon & Patrick Perré
LGPM, CentraleSupélec, Université Paris-Saclay, SFR Condorcet FR CNRS 3417,
Centre Européen de Biotechnologie et de Bioéconomie (CEBB),
3 rue des Rouges Terres 51110 Pomacle, France

Abstract

This work provides a model and the associated set of parameters allowing for microalgae population growth computation under intermittent lightning. Han's model is coupled with a simple microalgae growth model to yield a relationship between illumination and population growth. The model parameters were obtained by fitting a dataset available in literature using Particle Swarm Optimization method. In their work, authors grew microalgae in excess of nutrients under flashing conditions. Light/dark cycles used for these experimentations are quite close to those found in photobioreactor, i.e. ranging from several seconds to one minute. In this work, in addition to producing the set of parameters, Particle Swarm Optimization robustness was assessed. To do so, two different swarm initialization techniques were used, i.e. uniform and random distribution throughout the search-space. Both yielded the same results. In addition, swarm distribution analysis reveals that the swarm converges to a unique minimum. Thus, the produced set of parameters can be trustfully used to link light intensity to population growth rate. Furthermore, the set is capable to describe photodamages effects on population growth. Hence, accounting for light overexposure effect on algal growth.
Keywords: Han's model, Light, Modeling, Population growth rate, Microalgae

1 Introduction

Microalgae growth is receiving increasing attention in the scope of producing biofuels or fixing atmospheric CO_2 [1, 2, 3, 4]. Two different experimental approaches coexists: open ponds and photobioreactors. The first ones deliver a cost effective high scale solution, at the price of low control over the growth conditions and a very high risk of contamination [5]. The second allows for a very tight control of operating conditions, while being expensive and scalable only with difficulty.

Because of their very controlled nature, photobioreactors are reasonable assumed to be perfectly stirred reactors regarding nutrients and dissolved gases concentrations [6, 7]. Regarding illumination inside of the reactor, it is well known that such an assumption cannot be drawn because of light attenuation [8, 9, 10]. Yet, light is key to microalgae growth. It is therefore a critical parameter when designing a photobioreactor.

In 2013, Béchet et al. [11] reviewed the currently available models for determining the amount of light received by a culture and its impact on algal growth. The existing models can be sorted out into three different categories:

- black boxes: they predict the total photosynthetic yield of a culture as a function of the total or averaged light intensity reaching the culture [12]. These models are very easy to handle. In addition, they allow for a simple 0D modeling approach. Nevertheless, their shortcomings are numerous, the most dramatic one is that they critically depend on the experimental data that have been used to calibrate them. Obviously, they can not account for light attenuation in the reactor.
- local light intensity models: they describe the attenuation of light throughout the reactor. Thus they allow for spatial integration of light and related growth rate distribution over the reactor volume. Usually, they can account for light attenuation based on cell density and cell pigment content [13]. They yield significantly better results than black boxes models. Nevertheless, they assume that microalgae response to light is always in steady state. Thus, they are not able to take into account dynamic temporal effects (light/dark cycle) inside of the reactor which is today known to have an important impact on microalgae behavior [14].
- mechanistic models: they describe the microalgae response to light in term of activation of the key proteins at stake in the photosynthetic process. Among them, Han's model [15] is nowadays widely used in the community [16, 17, 18, 19, 20]. It is an improvement of the firstly proposed model [21] which take into account photodamages due to light overexposure.

The model used to describe culture response to illumination has strong implications on the choice of the model describing algae motion inside of the reactor. While black boxes models work perfectly well with perfectly stirred reactor assumption. Mechanistic models would require to know the position of the microalgae inside of the reactor, and the corresponding illumination, to yield the full-extend of their power.

Han's model particularly well suited for photobioreactor numerical design. Indeed, using CFD capabilities, it is nowadays possible to access light pattern seen by tracers reproducing microalgae [22, 18]. Yet, assuming that light is the limiting growth factor, finding a tight set of Han's model parameters linking directly intermittent light exposure to growth rate is a difficult task. Most of the time, in literature, light supply is coupled with other nutrient limitations and population light adaptation strategy [20, 16, 23]. Hence, it is quite challenging to implement such models. Furthermore, such a complexity is not mandatory when solely light effects are to be investigated.

The aim of this work is to provided a set of parameter allowing for population growth computation, under nutrient excess assumption, as a time dynamic function of illumination. To do so, a dataset available in literature will be used [24]. In their work, authors grew microalgae in excess of nutrients under flashing conditions. Light/dark cycles used for these experimentations are quite close to those found in photobioreactor, i.e. ranging from several seconds to one minute [25, 26, 22]. In a second part of their work, the authors used an heavy mathematical treatment and assumption to use ordinary least square method to calibrate a model [27]. Even though their model is resembling to the widely popular Han's model, the parameters cannot be transposed. Thus in this work, Han's model parameter will be produced using Particle Swarm Optimization method.

2 Nomenclature

Latin symbols	
A	A state (open) of a photosynthetic unit, -
B	B state (processing) of a photosynthetic unit, -
C	C state (damaged) of a photosynthetic unit, -
D	diameter, m
F	cost function, -
I	light intensity, μmolQuanta/m^2/s
K	light to growth rate dimensionless constant, -
k_d	photosynthetic unit photodamage rate, μmolQuanta/m^2/s
k_r	photosynthetic unit repair rate, 1/s
l	length, m
Me	maintenance rate, 1/h
P	linear pumping power, W/m
Re	Reynolds number, $Re = \frac{DV}{\nu}$
t	time, s
t_i	illumination time, s
V	velocity, m/s

Greek symbols	
α	absorption coefficient, 1/m
μ	population growth rate, 1/h
ν	kinematic viscosity, m^2/s
rho	density, kg/m^3
σ	photosystem cross section, m^2/μmolQuanta
τ	turnover rate, 1/s

Subscripts	
exp	experimental observation
i	dummy index
$PSII$	PhotoSystem II
num	numerical prediction
sun	sun
$vortex$	turbulent vortex

3 Experimental dataset

In their original work, the authors grew Red Marine algae, Porphyridium sp. (UTEX637) in a photobioreactor (Fig. 1). Extensive description of the experimental procedure is available in [24]. In this work only the main features will be summarized. The reactor is mainly composed of two parts:

- a gas column with a sparger (elements 1 and 2 and Fig. 1), ensuring fluid motion through the reactor and CO_2 supply to the culture medium thanks to 3% CO_2 air bubbling

- a small diameter tube, where algae are exposed to light on the upper part of the tube (element 3 and Fig. 1), then travel thought a darkness in the lower of the tube (element 4 and Fig. 1)

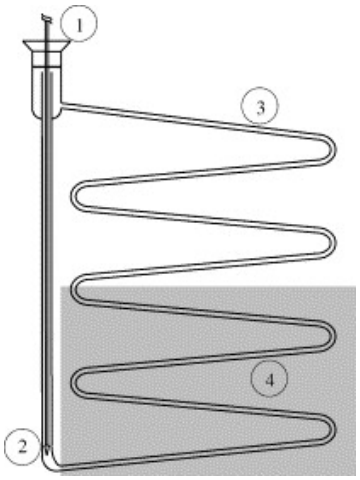

Figure 1: Scheme of the tubular loop reactor with air lift pump. (1) Gas inlet; (2) gas sparger (air+CO_2); (3) illuminated part of the tubular reactor; (4) dark part of the tubular reactor [24].

The average cycle time of algae around the reactor is 45 seconds. Illuminations time (t_i) can be adjusted by varying the length of the dark zone of the reactor. In this case, illumination time range between 45 seconds, i.e. constant illumination, down to 28.3 seconds. Hence an illumination proportion ranging from 63% to 100% over a constant period of 45 seconds.

Light intensity was set to three different values: 110, 220 and 550 μmolQuanta/m^2/s, referred as low, medium and high intensity lighting. The purpose the high intensity lighting was to trigger photodamage. In addition to using a small diameter tube, the authors took care to verify that no biofilm was developing on the tube surface. Hence, the lighting is uniform throughout the photobioreactor.

Population growth rate was monitored for 48 hours during the exponential growth phase by twice daily microscope cell count. Each experiment was repeated twice. Results can be found in Table 1. One can note the good repeatability of the results.

Light intensity	μ (h^{-1})						
(μmolQuanta/m^2/s)	t_i = 45 s	43.3 s	41.7 s	38.3 s	36.7 s	35 s	28.3 s
110	0.05022	-	0.04916	0.03513	0.03437	0.03397	0.01232
	0.05051	-	0.04196	0.04376	0.03914	0.03301	0.02292
220	0.05554	-	0.05369	0.05355	0.0501	0.04225	0.01883
	0.05665	-	0.0566	0.05628	0.04417	0.04046	0.02816
550	0.04457	0.05015	0.05437	0.05461	0.04403	0.0453	0.03326
	0.04346	0.05127	0.05645	0.0557	0.05662	0.03837	0.03209

Table 1: Population growth rate under different light intensities and exposure times [24].

4 Mathematical model

In their work, the authors used a nowadays outdated model [27]. Today, Han's mechanistic model has shown is robustness and is widely used. This model considers the photosynthetic system II as the bottleneck of the whole photosynthesis process, thus the limiting growth factor with respect to light. This system is seen as composed of proteins, or units, that can interact with photons (Fig. 2). Light interaction can be broken down into three states:

- open state: the unit is waiting for a photon to activate it. Once it captured a photon, it enters the *processing state*.
- processing state: the unit is processing the captured photon energy with characteristic time τ, called the turnover rate. Once the photon has been processed, the units returns to the *open state*. If, while processing a photon, the unit is hit by another photon the unit has a chance (k_d) to enter the *damaged state*.
- damaged state: once damaged, the photosynthetic unit takes a certain time ($1/k_r$) to repair itself. Afterwards, it returns to the *processing state*.

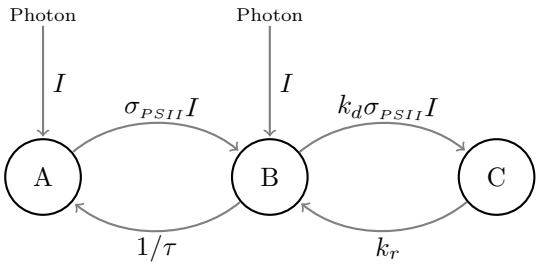

Figure 2: Han's model of the PhotoSystem II [15]. A: open state. B: processing state. C: damaged state.

$$\frac{dA}{dt} = -I\sigma_{PSII}A + \frac{B}{\tau} \tag{1}$$

$$\frac{dB}{dt} = I\sigma_{PSII}A - \frac{B}{\tau} + k_rC - k_dI\sigma_{PSII}B \tag{2}$$

$$\frac{dC}{dt} = k_dI\sigma_{PSII}B - k_rC \tag{3}$$

Mathematically, a balance over the different photosynthetic units states can be derived. It yields Han's model equation (Eq. 1 to 3). In addition, one should note that $A + B + C = 1$. In order to go one step further, it is possible to link the photosynthetic unit state to population growth under the assumption that light is the limiting growth factor. With given units, i.e. μ in per hour, τ in seconds and Me in per hour, the equation governing population growth rate can be expressed as Eq. 4:

$$\mu = 3600K\frac{B}{\tau} - Me \tag{4}$$

5 Optimization procedure

The model parameters (σ_{PSII}, τ, k_d, k_r, K, Me) were determined using Particle Swarm Optimization method. This method was originally derived from the observation of animal groups behavior [28, 29]. Each particle tends to explore the search-space ballistically. Yet, in its search, it takes account its own history (i.e. the minimum it found, thought memory mechanism) and the whole swarm history (i.e. the swarm minimum, thought a social mechanism). Its mathematical relevance has been shown in cases requiring the optimization of numerous parameters [30]. This method has already been successfully used to solve various problem (building cost optimization, solar power plant design, ... [31, 32]) including some with highly discontinuous cost functions [33]. Particle Swarm Optimization algorithms are defined mainly by the relative weights of their three different mechanisms: interia, memory and socialization. In our case, the weights of those parameters were set to 0.6, 1 and 1 respectively, following the work of [34] where 0.6 inertia weight gave the fastest convergence on average.

The optimization procedure aims at minimizing the cost function, in this case the relative gap between the numerical predicted population growth rate values ($\mu_{num,i}$) with a given set of parameters and the experimentally reported values ($\mu_{exp,i}$) (Eq. 5). For every set of parameters evaluated by the optimization algorithm, the numerical predicted population growth rate ($\mu_{num,i}$) was obtained by solving Han's model until it reaches a pseudo-steady state. The time integration routine used a timestep converged backward Euler scheme. The search for the minimum was stop after the swarm minimum did not evolved for 100 iterations of a value higher than 0.01% of this minimum value.

The search space for the six parameters was defined based very widened literature range for parameter values (Tab. 2) [20, 16], whenever possible. In order to assess for the reliability, two types of swarm initialization were used: uniform spreading and random spreading throughout the search space [35]. In both cases, one million particles were used to roam the search-space.

$$F = \sum_{i=1}^{n}\left(\frac{\mu_{num,i} - \mu_{exp,i}}{\mu_{num,i} + \mu_{exp,i}}\right)^2 \tag{5}$$

6 Results and discussion

Parameters determined by the two optimization runs can be found in Table 2. The two sets of parameters are very close, discrepancies arise after 3 significant digits. They are considered to be identical. The uniformly initialized algorithm converged faster (26 iterations) than the randomly initialized one (69 iterations). Yet, this difference is attributed to the stochastic component of the swarm behavior. Figure 3 presents the swarm distribution in the search-space after 126 iterations. One can see that the swarm converges towards a single set of parameters.

Parameter	σ_{PSII} (m^2/μmolQuanta)	τ (s)	k_d (-)	k_r (s^{-1})	K (-)	Me (h^{-1})
Search space	10^{-4} - 10^{2}	10^{-2} - 10^{2}	10^{-6} - 10^{-1}	10^{-6} - 10^{-1}	10^{-3} - 10^{2}	10^{-3} - 10^{0}
Uniform†	$3.85\ 10^{-3}$	$2.81\ 10^{1}$	$3.95\ 10^{-4}$	$1.32\ 10^{-2}$	$8.57\ 10^{0}$	$2.30\ 10^{-1}$
Random†	$3.85\ 10^{-3}$	$2.81\ 10^{1}$	$3.95\ 10^{-4}$	$1.32\ 10^{-2}$	$8.57\ 10^{0}$	$2.30\ 10^{-1}$

Table 2: Optimized parameters for Han's model. † Swarm initialization method.

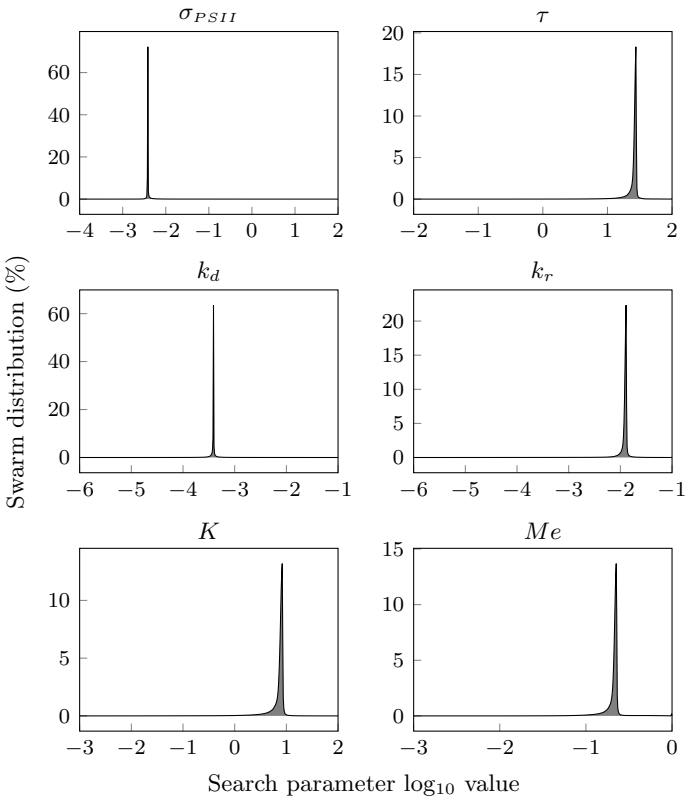

Figure 3: Particle swarm distribution throughout the search-space after 126 iterations, including 100 iterations of stagnation. Uniform initialization.

Figure 4 reports numerically predicted and experimentally observed population growth rates. Using the optimized set of parameters, the model captures well the population growth rates under low and medium light intensities. Under high intensity, the model is capable of reproducing the trends followed by the population growth rate, hence accounting for photoinhibition. Yet quantitative discrepancies arise. They can be explained by the fact that the experimental dataset is skewed towards conditions where photodamages do not occur, i.e. low and medium light intensities. Nevertheless, the qualitative phenomenon is well described.

Figure 5 presents the proportion of photodamaged photosynthetic units, in pseudo steady state, when exposed to different light intensities and illumination times. One can see that the exposure time has a limited impact on the quantity of photodamaged units. On the contrary, it increases almost linearly with the incident light intensity. This can be explained by the low value of k_r parameters. Indeed, $1/k_r < 45$ s, thus, the damaged units cannot fully repair themselves over the course of the dark part of the cycle.

Figure 6 presents an example of response of photosynthetic unit under a given light and intensity. One can see that, in pseudo steady state, the second photosynthetic system requires around 10 seconds to reach its full capacities when entering the lighted phase. On the opposite, the system has not enough time to stabilize itself over the dark phase (16.7 s). With regards to the light characteristic times at stake in photobioreactors (several second to 1 minute), this shows that the assumption of steady state light response, sometimes made in literature, is quite strong.

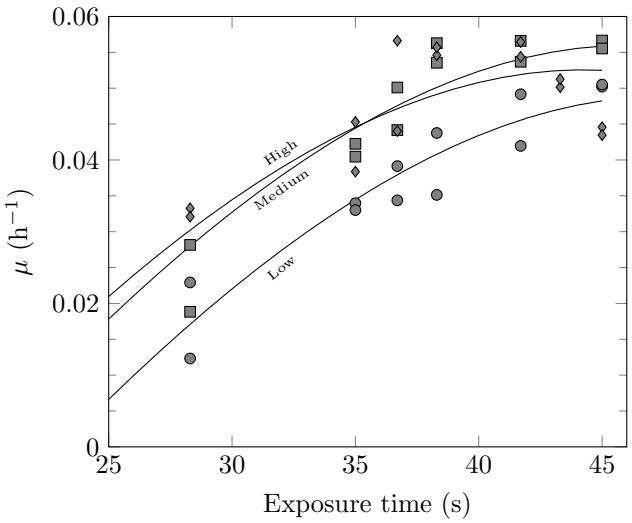

Figure 4: Numerical predicted and experimentally observed population growth rates, for different illumination times under different light intensities. Continuous lines: model predictions. Circle marks: experimental observations under low intensity. Square marks: experimental observations under medium intensity. Diamond marks: experimental observations under high intensity.

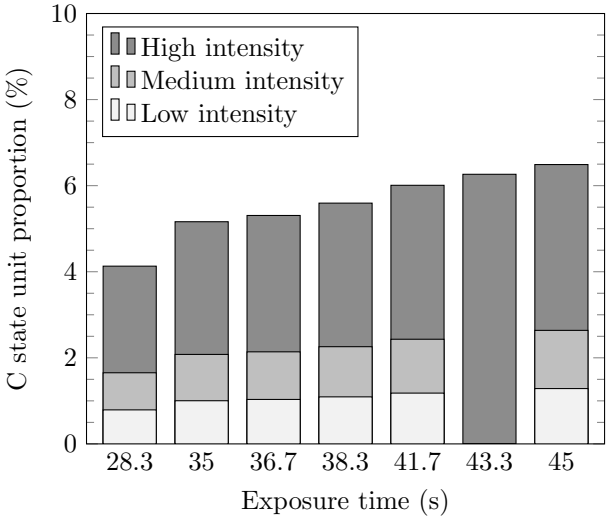

Figure 5: Proportion of C state (photodamaged) PhotoSynthetic Units II in response to light cycles, for different illumination times under different light intensities. Note: data were not available for low and medium intensities for a cycle duration of 43.3 s.

7 Application to a tubular photobioreactor

In order to illustrate the potential applications of the proposed set of parameters, we will consider an outdoor tubular photobioreactor [36, 37, 38]. The considered design is freely inspired from [36], because this study provides a map of the illumination across the growth medium sectio (Fig. 7). In the case of real outdoor applications, illumination variates across the day following the path of the sun. Hence, illumination rises from nothing at dawn up to values as high as 1000 μmolQuanta/m^2/s at midday before fading away at dusk. In this case, the maximum light intensity is very likely to induce photodamages. To alleviate this problem, the tubings (2 m for each part, diameter 6 cm) will alternate parts exposed to the sun, where microalgae can capture the light, grow and may experience photodamages, and parts covered from the sun, where they can recover(Fig. 8).

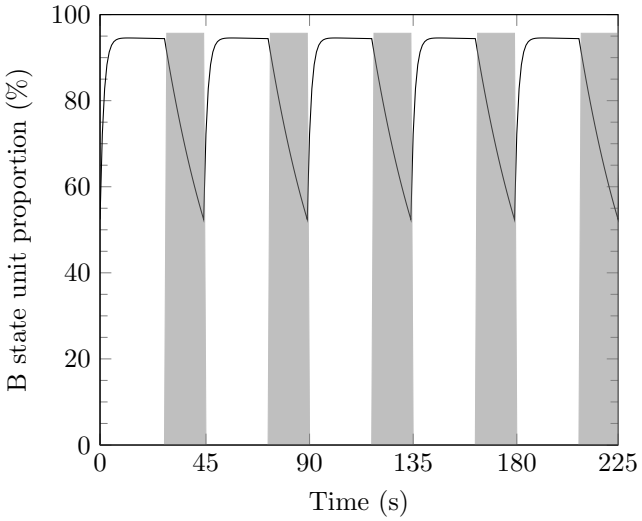

Figure 6: Proportion of B state PhotoSynthetic Units II in response to light cycles, in pseudo steady state. Dark part of the cycle in gray. Light intensity: 220 μmolQuanta/m^2/s, exposure time: 28.3 s.

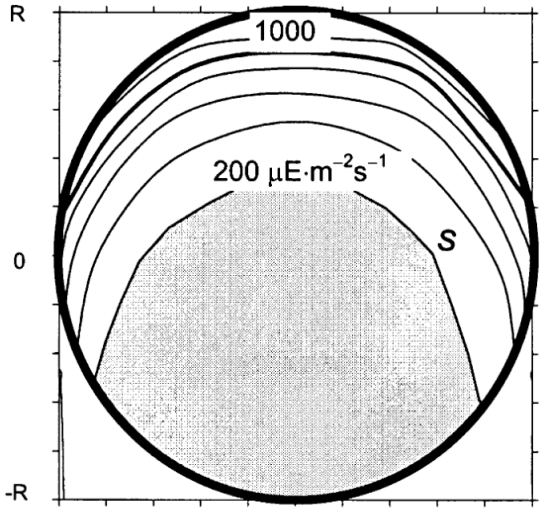

Figure 7: Illumination map across the tube section at midday [36]. Tube diameter: 6cm.

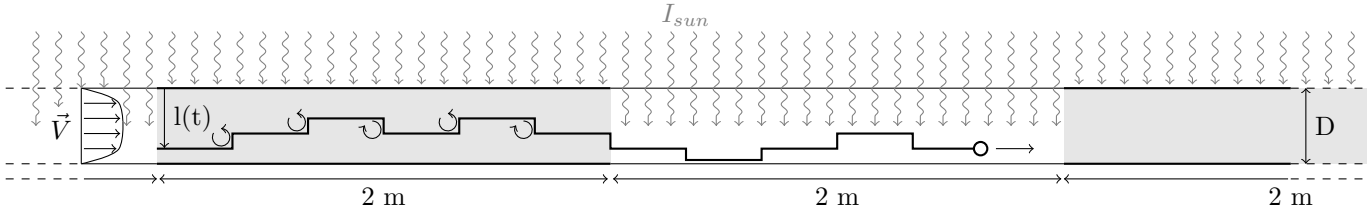

Figure 8: Schematic of a fraction of the tubular photobioreactor. Gray areas: sun covered parts. White areas: sun exposed parts. Curvy arrows: incident light. Broken black line: one microalgae trajectory example.

7.1 Operating conditions

In order to ensure that all the microalgae population is growing under proper conditions, two parameters are of importance: dilution rate and flow regime. The reactor is considered operated in such a way that the dilution rate ensure that at least 90 % of the incident light is absorbed by the culture. The flow has to be turbulent (i.e. Re $>$ 2300) because it ensures a good mixing as well as help preventing reactor from fouling.

7.2 Population growth model

In order to investigate the reactor performances, population growth has to be modeled. To do so, 100 tracers are followed during their circulation throughout the reactor. The growth conditions - illumination with time - of each tracer can be obtained thank to simple physical considerations on turbulent flows.

Let's assume that a tracer is at the center of the tube. It is submitted to two phenomena: convection by the growth medium at a velocity V and radial motion because of vortices originating from the turbulence (see tracer trajectory on Fig. 8). As a good rule of thumb, one can assume that vortices magnitude is about 10 % of the tube diameter and that vortices velocity are about 10 % of the flow velocity. Given the fact that the flow is turbulent, it is possible to reasonably assume that the velocity is uniform over the tube radius. Hence it is possible to deduce the hydrodynamic characteristic time (Eq. 6).

$$t_{vortex} = \frac{10\%D}{10\%V} \tag{6}$$

Using a random march approach, it is possible to produce the trajectory of a tracer throughout the tube and to know its distance from the illuminated side of the tube. Thus, applying Beer-Lambert law (Eq. 7) perceived illumination can be computed (Fig. 9). Finally individual growth rate can be computed using the model presented in Section 4. Tracer circulation is simulated until its mean growth rate stabilizes. Then, the 100 tracers individual growth rates are averaged to obtain the population average growth rate.

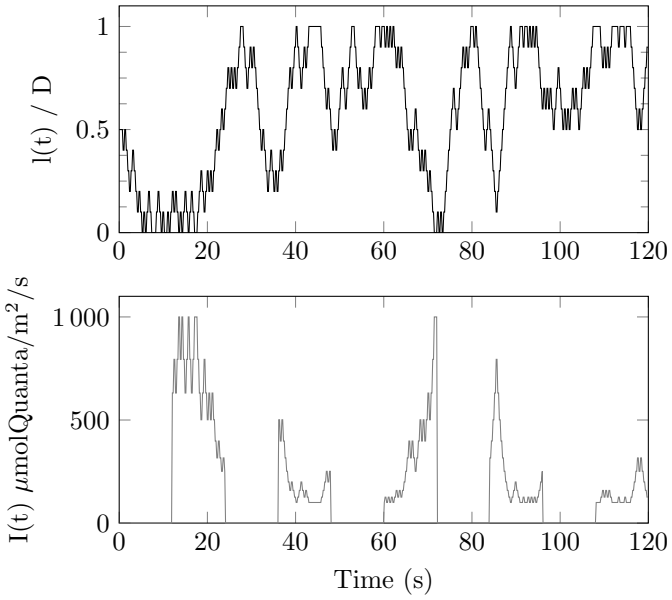

Figure 9: Sampling of one tracer random march. Upper figure: tracer distance to the illuminated side. Lower figure: perceived illumination. I_{sun} = 1000 μmolQuanta/m^2/s.

$$I(t) = I_{sun} exp(-\alpha\ l(t)) \tag{7}$$

With α (absorption coefficient) being deduced from the fact for $l = D$, $I(D) = 0.10 I_{sun}$, thus:

$$\alpha = \frac{-ln(\frac{I(D)}{I_{sun}})}{D} = 38\ m^{-1} \tag{8}$$

7.3 Performances investigation

As it can be derived from the previous model, liquid velocity plays an important role in determining the population growth rate because it dominates illumination patterns. Yet, a question arises, given the fact that liquid pumping costs power, what is the optimal velocity inside of the reactor ? In order to investigate this problem, the average population growth is computed under three different illuminations: midday (1000 μmolQuanta/m^2/s), morning and afternoon (500 μmolQuanta/m^2/s) and dawn and dusk (250 μmolQuanta/m^2/s) for Reynolds number ranging from 3000 to 35000.

Figure 10 presents the population averaged growth under the three different illuminations. The three curves exhibit the same trend. They increase dramatically for values of Reynolds number between 3000 and 10000. Once a Reynolds number of 20000 is reached, they increase linearly. This figure also highlights the non linear response to light intensity. For example, at a given Reynolds of 20000, increasing the amount of light from 250 to 500 μmolQuanta/m^2/s induces a rise of the growth rate from 0.013 to 0.032 h^{-1}. Yet, increasing the illumination up to 1000 μmolQuanta/m^2/s only lead to a population growth rate

of 0.040 h^{-1}. This nonlinear pattern can be explained by a saturation of the photosynthetic system (Section 4) which does not respond linearly to incident light intensity. Indeed, on average, 19 % of the photosynthetic units are in open state (or A state) for an illumination of 250 μmolQuanta/m^2/s, while only 10 and 5 % for 500 and 1000 μmolQuanta/m^2/s illuminations respectively.

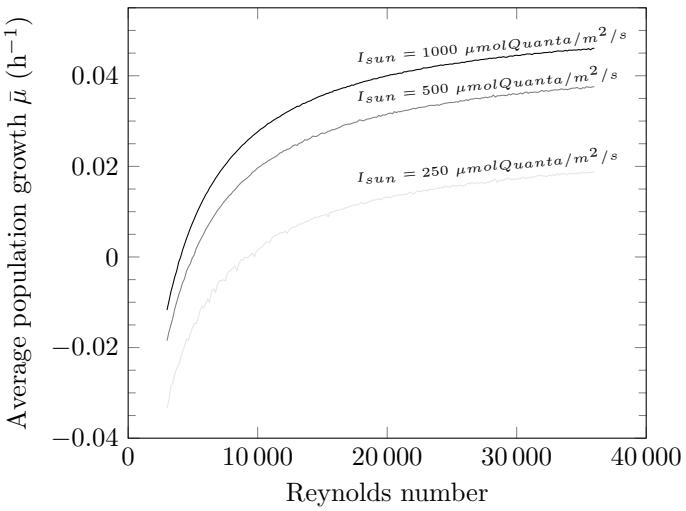

Figure 10: Population averaged growth for the three different illuminations.

From Figure 10h, it can be concluded that the higher the velocity the higher the biomass yield. Yet, one should take into account the pumping cost that does not increase linearly with Reynolds number. In order to go one step further, the pumping power, and in fine cost, can be estimated using Blasius' friction factor for smooth pipes (Eq. 9, where P is the linear pumping cost in W/m).

$$P = \frac{1}{2}\frac{0.3164}{Re^{0.25}}\frac{\rho V^2}{D} \tag{9}$$

Figure 11 reports the population averaged growth rate divided by the linear pumping power. The trend is the same for the three studied illumination: the sharp peak followed by a long downward slope. The peak location corresponds to the best compromise between algal growth and pumping cost for a given illumination. As one can see on the graph, the optimal Reynolds number depends on the illumination. Optimal values are 5400, 6600 and 12600 for 1000, 500 and 250 μmolQuanta/m^2/s respectively. Hence for an optimal operation of this reactor, it is advisable to adjust the circulating flowrate over the course of a day.

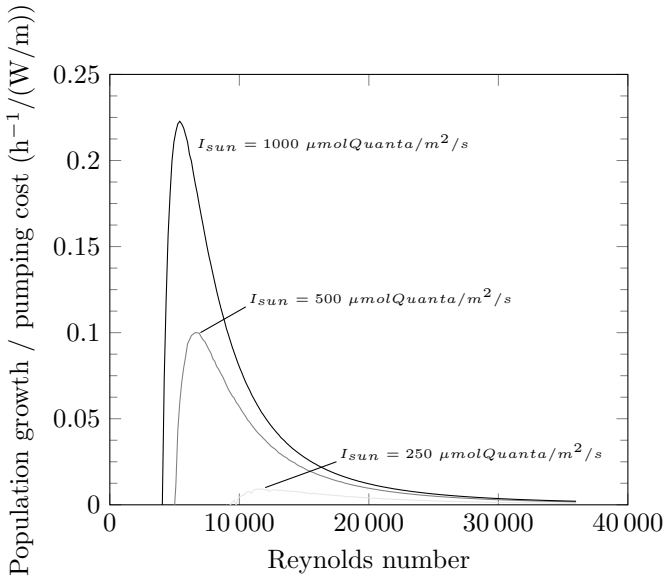

Figure 11: Population averaged growth divided by the pumping power for the three different illuminations.

8 Conclusion

The aim of this work was to provide a set of Han's model parameters in order to use it for photobioreactor design purposes. The experimental dataset was obtained from Red Marine algae, Porphyridium sp. (UTEX637) cultures. These algae were grown under different light cycles and intensities, with 3%CO_2 bubbling air. The light cycles used to grow algae have the same order of magnitude as the light characteristic time that can be found in photobioreactors.

Han's model parameters were determined using Particle Swarm Optimization procedure. Two different swarm initialization techniques were used, i.e. uniform and random distribution throughout the search-space. Both yielded the same results. In addition, swarm distribution analysis reveals that the swarm converges to a unique minimum. The produced set of parameters can be used to link light intensity to population growth rate. Furthermore, the set is capable to describe photodamages effects on population growth. Hence, accounting for light overexposure effect on algal growth.

With this work, a tight set of Han's model parameters has been delivered. It is readily usable for describing light influence on population growth in photobioreactor. It was successfully applied to the design of a tubular photobioreactor, providing insight on an optimized operating protocol. Even though, one can expect the values of the parameter to be species dependent, to some extend, the application of the provided set has shown, in the scope of understanding general behavior in a photobioreactor, that it could already yield valuable insights.

References

[1] J. Quinn, L. de Winter, T. Bradley, Microalgae bulk growth model with application to industrial scale systems, Bioresource Technology 102 (8) (2011) 5083–5092. doi:10.1016/j.biortech.2011.01.019.
URL http://www.sciencedirect.com/science/article/pii/S0960852411000654

[2] C.-Y. Chen, K.-L. Yeh, R. Aisyah, D.-J. Lee, J.-S. Chang, Cultivation, photobioreactor design and harvesting of microalgae for biodiesel production: A critical review, Bioresource Technology 102 (1) (2011) 71–81. doi:10.1016/j.biortech.2010.06.159.
URL http://www.sciencedirect.com/science/article/pii/S0960852410011648

[3] J. Yang, E. Rasa, P. Tantayotai, K. M. Scow, H. Yuan, K. R. Hristova, Mathematical model of Chlorella minutissima UTEX2341 growth and lipid production under photoheterotrophic fermentation conditions, Bioresource Technology 102 (3) (2011) 3077–3082. doi:10.1016/j.biortech.2010.10.049.
URL http://www.sciencedirect.com/science/article/pii/S0960852410017050

[4] A. Packer, Y. Li, T. Andersen, Q. Hu, Y. Kuang, M. Sommerfeld, Growth and neutral lipid synthesis in green microalgae: A mathematical model, Bioresource Technology 102 (1) (2011) 111–117. doi:10.1016/j.biortech.2010.06.029.
URL http://www.sciencedirect.com/science/article/pii/S0960852410010102

[5] R. E. Davis, D. B. Fishman, E. D. Frank, M. C. Johnson, S. B. Jones, C. M. Kinchin, R. L. Skaggs, E. R. Venteris, M. S. Wigmosta, Integrated Evaluation of Cost, Emissions, and Resource Potential for Algal Biofuels at the National Scale, Environmental Science & Technology 48 (10) (2014) 6035–6042. doi:10.1021/es4055719.
URL http://dx.doi.org/10.1021/es4055719

[6] J. P. Bitog, I. B. Lee, C. G. Lee, K. S. Kim, H. S. Hwang, S. W. Hong, I. H. Seo, K. S. Kwon, E. Mostafa, Application of computational fluid dynamics for modeling and designing photobioreactors for microalgae production: A review, Computers and Electronics in Agriculture 76 (2) (2011) 131–147. doi:10.1016/j.compag.2011.01.015.
URL http://www.sciencedirect.com/science/article/pii/S0168169911000305

[7] M. R. Rampure, A. A. Kulkarni, V. V. Ranade, Hydrodynamics of Bubble Column Reactors at High Gas Velocity: Experiments and Computational Fluid Dynamics (CFD) Simulations, Industrial & Engineering Chemistry Research 46 (25) (2007) 8431–8447. doi:10.1021/ie070079h.
URL http://dx.doi.org/10.1021/ie070079h

[8] E. M. Grima, F. G. Camacho, J. A. S. Pérez, J. M. F. Sevilla, F. G. A. Fernández, A. C. Gómez, A mathematical model of microalgal growth in light-limited chemostat culture, Journal of Chemical Technology & Biotechnology 61 (2) (1994) 167–173. doi:10.1002/jctb.280610212.
URL http://onlinelibrary.wiley.com/doi/10.1002/jctb.280610212/abstract

[9] O. Bernard, Hurdles and challenges for modelling and control of microalgae for CO2 mitigation and biofuel production, Journal of Process Control 21 (10) (2011) 1378–1389. doi:10.1016/j.jprocont.2011.07.012.
URL http://www.sciencedirect.com/science/article/pii/S0959152411001533

[10] A. Bernardi, A. Nikolaou, A. Meneghesso, T. Morosinotto, B. Chachuat, F. Bezzo, High-Fidelity Modelling Methodology of Light-Limited Photosynthetic Production in Microalgae, PLOS ONE 11 (4) (2016) e0152387. doi:10.1371/journal.pone.0152387.
URL http://journals.plos.org/plosone/article?id=10.1371/journal.pone.0152387

[11] Q. Béchet, A. Shilton, B. Guieysse, Modeling the effects of light and temperature on algae growth: State of the art and critical assessment for productivity prediction during outdoor cultivation, Biotechnology Advances 31 (8) (2013) 1648–1663. doi:10.1016/j.biotechadv.2013.08.014.
URL http://www.sciencedirect.com/science/article/pii/S0734975013001481

[12] H. L. MacIntyre, T. M. Kana, T. Anning, R. J. Geider, Photoacclimation of Photosynthesis Irradiance Response Curves and Photosynthetic Pigments in Microalgae and Cyanobacteria1, Journal of Phycology 38 (1) (2002) 17–38. doi:10.1046/j.1529-8817.2002.00094.x.
URL http://onlinelibrary.wiley.com/doi/10.1046/j.1529-8817.2002.00094.x/abstract

[13] D. Undurraga, P. Poirrier, R. Chamy, Microalgae growth kinetic model based on the PSII quantum yield and its utilization in the operational curves construction, Algal Research 17 (2016) 330–340. doi:10.1016/j.algal.2016.05.020.
URL http://www.sciencedirect.com/science/article/pii/S221192641630176X

[14] S. Abu-Ghosh, D. Fixler, Z. Dubinsky, D. Iluz, Flashing light in microalgae biotechnology, Bioresource Technology 203 (2016) 357–363. doi:10.1016/j.biortech.2015.12.057.
URL http://www.sciencedirect.com/science/article/pii/S0960852415016879

[15] B.-P. HAN, A Mechanistic Model of Algal Photoinhibition Induced by Photodamage to Photosystem-II, Journal of Theoretical Biology 214 (4) (2002) 519–527. doi:10.1006/jtbi.2001.2468.
URL http://www.sciencedirect.com/science/article/pii/S0022519301924683

[16] S. Esposito, V. Botte, D. Iudicone, M. Ribera d'Alcala', Numerical analysis of cumulative impact of phytoplankton photoresponses to light variation on carbon assimilation, Journal of Theoretical Biology 261 (3) (2009) 361–371. doi:10.1016/j.jtbi.2009.07.032.
URL http://www.sciencedirect.com/science/article/pii/S0022519309003476

[17] P. Hartmann, Q. Béchet, O. Bernard, The effect of photosynthesis time scales on microalgae productivity, Bioprocess and Biosystems Engineering 37 (1) (2013) 17–25. doi:10.1007/s00449-013-1031-2.
URL http://link.springer.com/article/10.1007/s00449-013-1031-2

[18] P. Hartmann, D. Demory, C. Combe, R. Hamouda, A.-C. Boulanger, M.-O. Bristeau, J. Sainte-Marie, B. Sialve, J.-P. Steyer, S. Rabouille, Growth Rate Estimation of algae in Raceway Ponds: A novel Approach, in: The 19th World Congress of the International Federation of Automatic Control, 2014.

[19] A. Nikolaou, P. Hartmann, A. Sciandra, B. Chachuat, O. Bernard, Dynamic coupling of photoacclimation and photoinhibition in a model of microalgae growth, Journal of Theoretical Biology 390 (2016) 61–72. doi:10.1016/j.jtbi.2015.11.004.
URL http://www.sciencedirect.com/science/article/pii/S0022519315005408

[20] M. Baklouti, V. Faure, L. Pawlowski, A. Sciandra, Investigation and sensitivity analysis of a mechanistic phytoplankton model implemented in a new modular numerical tool (Eco3m) dedicated to biogeochemical modelling, Progress in Oceanography 71 (1) (2006) 34–58. doi:10.1016/j.pocean.2006.05.003.
URL http://www.sciencedirect.com/science/article/pii/S0079661106000772

[21] B.-P. HAN, Photosynthesis–Irradiance Response at Physiological Level: a Mechanistic Model, Journal of Theoretical Biology 213 (2) (2001) 121–127. doi:10.1006/jtbi.2001.2413.
URL http://www.sciencedirect.com/science/article/pii/S0022519301924130

[22] T. Sato, D. Yamada, S. Hirabayashi, Development of virtual photobioreactor for microalgae culture considering turbulent flow and flashing light effect, Energy Conversion and Management 51 (6) (2010) 1196–1201. doi:10.1016/j.enconman.2009.12.030.
URL http://www.sciencedirect.com/science/article/pii/S0196890409005366

[23] R. J. Geider, H. L. MacIntyre, T. M. Kana, A dynamic regulatory model of phytoplanktonic acclimation to light, nutrients, and temperature, Limnology and Oceanography 43 (4) (1998) 679–694.

[24] X. Wu, J. C. Merchuk, A model integrating fluid dynamics in photosynthesis and photoinhibition processes, Chemical Engineering Science 56 (11) (2001) 3527–3538. doi:10.1016/S0009-2509(01)00048-3.
URL http://www.sciencedirect.com/science/article/pii/S0009250901000483

[25] M. J. Barbosa, M. Janssen, N. Ham, J. Tramper, R. H. Wijffels, Microalgae cultivation in air-lift reactors: Modeling biomass yield and growth rate as a function of mixing frequency, Biotechnology and Bioengineering 82 (2) (2003) 170–179. doi:10.1002/bit.10563.
URL http://onlinelibrary.wiley.com/doi/10.1002/bit.10563/abstract

[26] M. Janssen, T. C. Kuijpers, B. Veldhoen, M. B. Ternbach, J. Tramper, L. R. Mur, R. H. Wijffels, Specific growth rate of Chlamydomonas reinhardtii and Chlorella sorokiniana under medium duration light/dark cycles: 13–87 s, Journal of Biotechnology 70 (1–3) (1999) 323–333. doi:10.1016/S0168-1656(99)00084-X.
URL http://www.sciencedirect.com/science/article/pii/S016816569900084X

[27] P. H. C. Eilers, J. C. H. Peeters, A model for the relationship between light intensity and the rate of photosynthesis in phytoplankton, Ecological Modelling 42 (3) (1988) 199–215. doi:10.1016/0304-3800(88)90057-9.
URL http://www.sciencedirect.com/science/article/pii/0304380088900579

[28] R. Eberhart, J. Kennedy, A new optimizer using particle swarm theory, in: , Proceedings of the Sixth International Symposium on Micro Machine and Human Science, 1995. MHS '95, 1995, pp. 39–43. doi:10.1109/MHS.1995.494215.

[29] C. W. Reynolds, Flocks, Herds and Schools: A Distributed Behavioral Model, in: Proceedings of the 14th Annual Conference on Computer Graphics and Interactive Techniques, SIGGRAPH '87, ACM, New York, NY, USA, 1987, pp. 25–34. doi:10.1145/37401.37406.
URL http://doi.acm.org/10.1145/37401.37406

[30] P. Andras, A Bayesian Interpretation of the Particle Swarm Optimization and Its Kernel Extension, PLoS ONE 7 (11) (2012) e48710. doi:10.1371/journal.pone.0048710.
URL http://dx.plos.org/10.1371/journal.pone.0048710

[31] A. Banks, J. Vincent, C. Anyakoha, A review of particle swarm optimization. Part II: hybridisation, combinatorial, multicriteria and constrained optimization, and indicative applications, Natural Computing 7 (1) (2007) 109–124. doi:10.1007/s11047-007-9050-z.
URL http://link.springer.com/article/10.1007/s11047-007-9050-z

[32] O. Farges, Conception optimale de centrales solaires à concentration : application aux centrales à tour et aux installations "beam down", phdthesis, Ecole des Mines d'Albi-Carmaux (Jun. 2014).
URL https://tel.archives-ouvertes.fr/tel-01135529/document

[33] M. Wetter, J. Wright, A comparison of deterministic and probabilistic optimization algorithms for nonsmooth simulation-based optimization, Building and Environment 39 (8) (2004) 989–999. doi:10.1016/j.buildenv.2004.01.022.
URL http://www.sciencedirect.com/science/article/pii/S0360132304000332

[34] Y. Shi, R. C. Eberhart, Parameter selection in particle swarm optimization, in: Evolutionary Programming VII, Lecture Notes in Computer Science, Springer, Berlin, Heidelberg, 1998, pp. 591–600. doi:10.1007/BFb0040810.
URL https://link.springer.com/chapter/10.1007/BFb0040810

[35] I. C. Trelea, The particle swarm optimization algorithm: convergence analysis and parameter selection, Information Processing Letters 85 (6) (2003) 317–325. doi:10.1016/S0020-0190(02)00447-7.
URL http://www.sciencedirect.com/science/article/pii/S0020019002004477

[36] E. Molina, J. Fernández, F. G. Acién, Y. Chisti, Tubular photobioreactor design for algal cultures, Journal of Biotechnology 92 (2) (2001) 113–131. doi:10.1016/S0168-1656(01)00353-4.
URL http://www.sciencedirect.com/science/article/pii/S0168165601003534

[37] J. A. Del Campo, H. Rodrı?guez, J. Moreno, M. Á. Vargas, J. Rivas, M. G. Guerrero, Lutein production by Muriellopsis sp. in an outdoor tubular photobioreactor, Journal of Biotechnology 85 (3) (2001) 289–295. doi:10.1016/S0168-1656(00)00380-1.
URL http://www.sciencedirect.com/science/article/pii/S0168165600003801

[38] G. Chini Zittelli, F. Lavista, A. Bastianini, L. Rodolfi, M. Vincenzini, M. R. Tredici, Production of eicosapentaenoic acid by Nannochloropsis sp. cultures in outdoor tubular photobioreactors, Journal of Biotechnology 70 (1) (1999) 299–312. doi:10.1016/S0168-1656(99)00082-6.
URL http://www.sciencedirect.com/science/article/pii/S0168165699000826